

2 Supplementary Material

3 Novel Oxygen Optode Sensor with Fast Response 4 Time: In-Depth Characterization and Assessment of 5 the HydroFlash O₂ Applicable for Several Ocean 6 Observing Platforms

7 Tobias Hahn* and Arne Körtzinger

8 *Correspondence:
9 Tobias Hahn
10 thahn@geomar.de

1 SUPPLEMENTARY FIGURES

11 1.1 O₂ & Temperature Dependence and Calibration: Accuracy, Precision

12 Exemplary calibration results for 4330 and HydroFlash O₂ optodes are shown in the following figures.
13 1.1.1 AADI 4330 Optodes

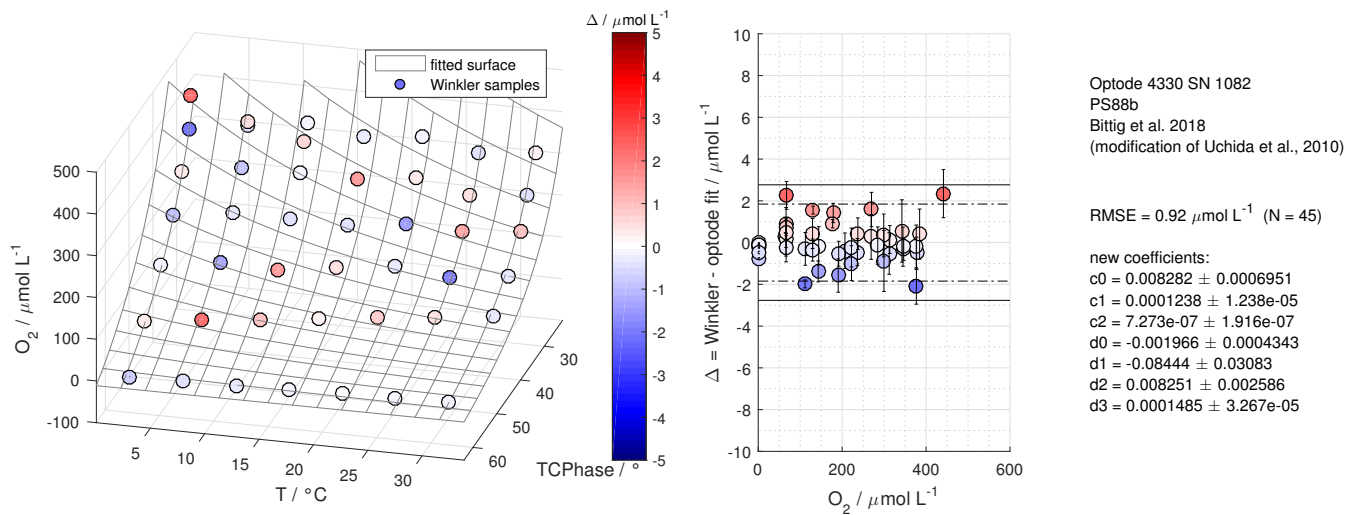


Figure S1: Calibration results of 4330-1082 from multi-point calibration 1

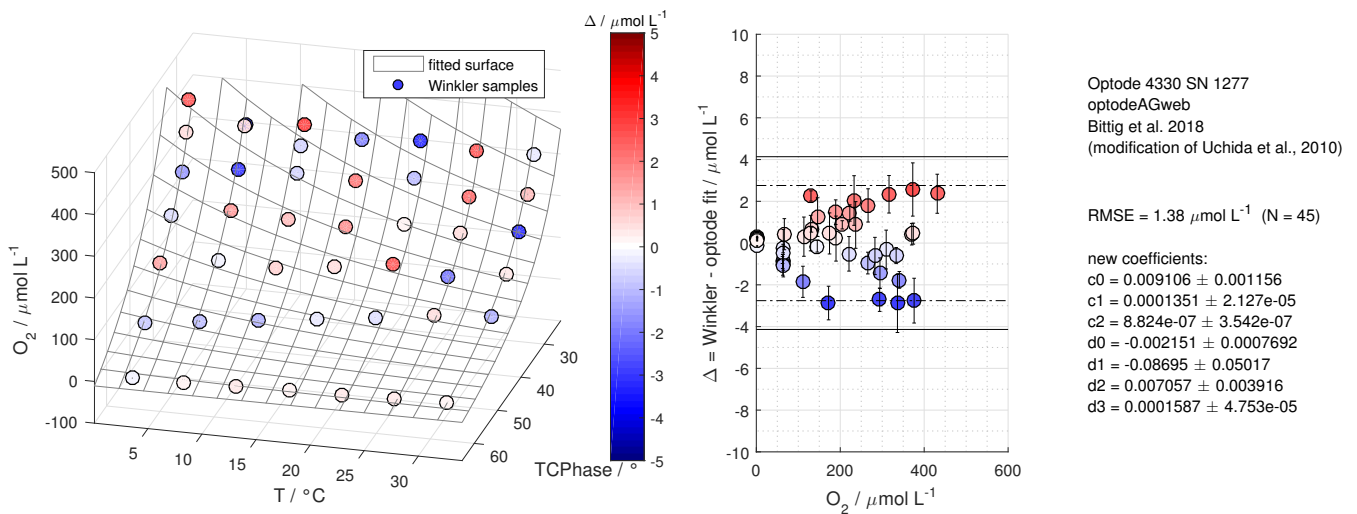


Figure S2: Calibration results of 4330-1277 from multi-point calibration 2

14 1.1.2 CONTROS HydroFlash® O₂ Optodes

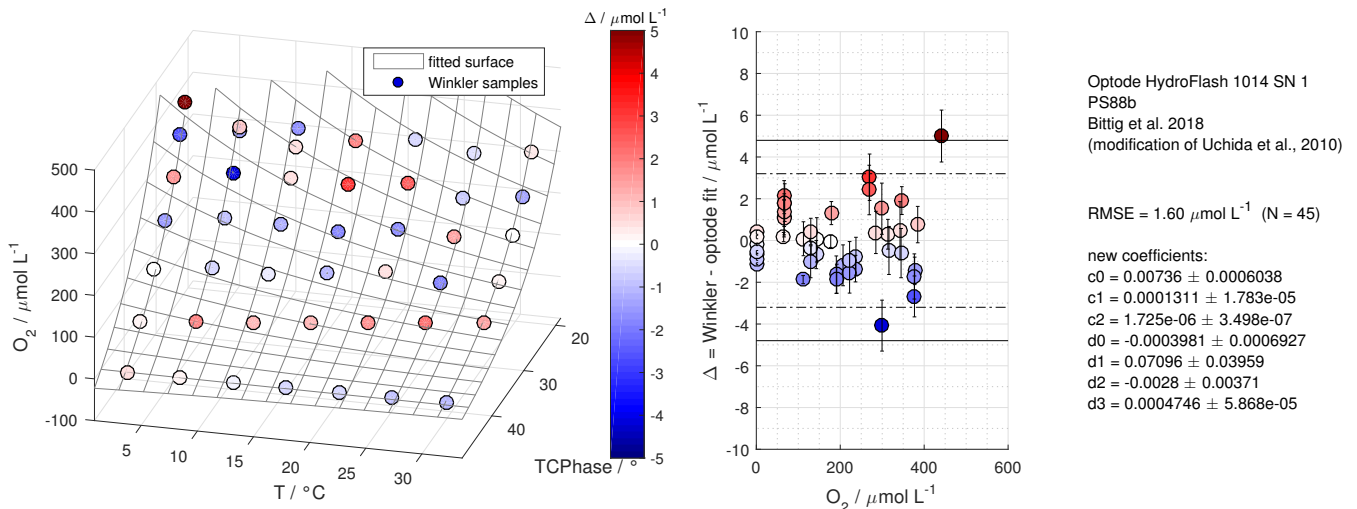


Figure S3: If the $3 \times \text{RMSE}$ criterion was exceeded, we considered the calibration results with the respective amount of calibration points (*here*: HF14-01 with n = 45 from multi-point calibration 1) as invalid.

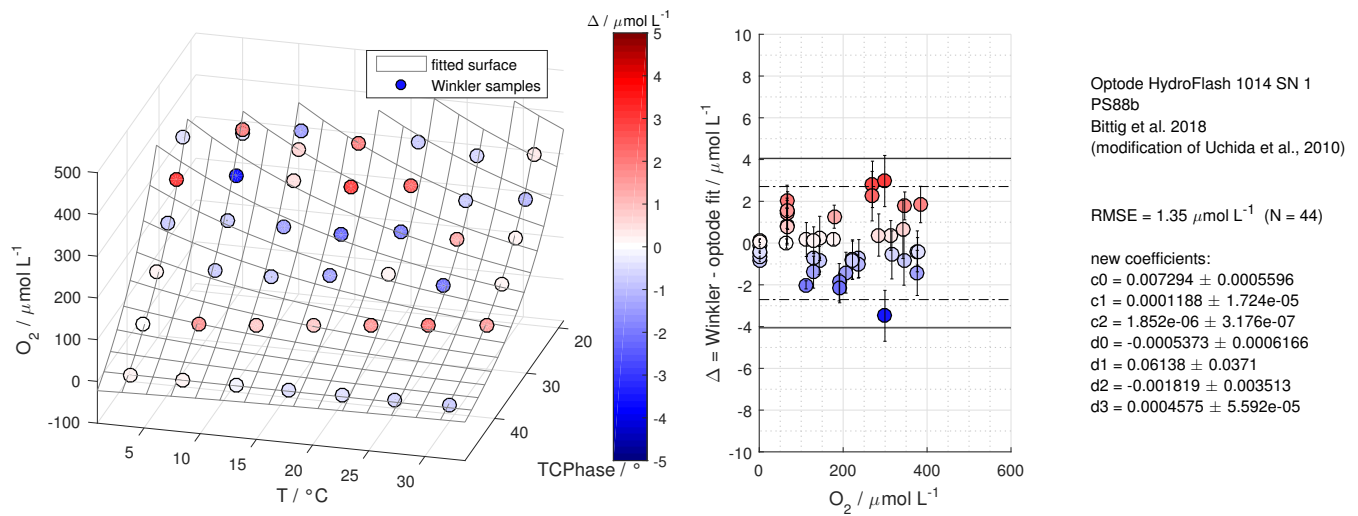


Figure S4: Calibration results of HF14-01 from multi-point calibration 1 without exceeding the 3xRMSE criterion

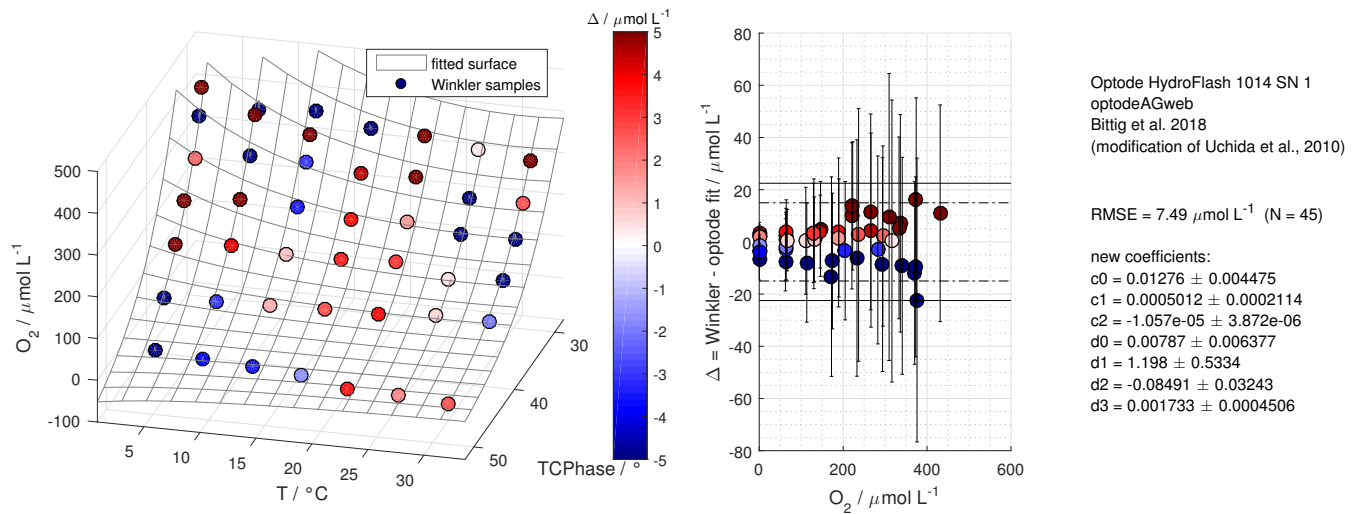


Figure S5: Calibration results of HF14-01 from multi-point calibration 2. This optode's sensor spot was damaged expressing in much higher misfit and RMSE between the reference and optode.

15 1.2 0% and 100% O₂ Calibration: Re-adjustments

16 1.2.1 From laboratory experiments

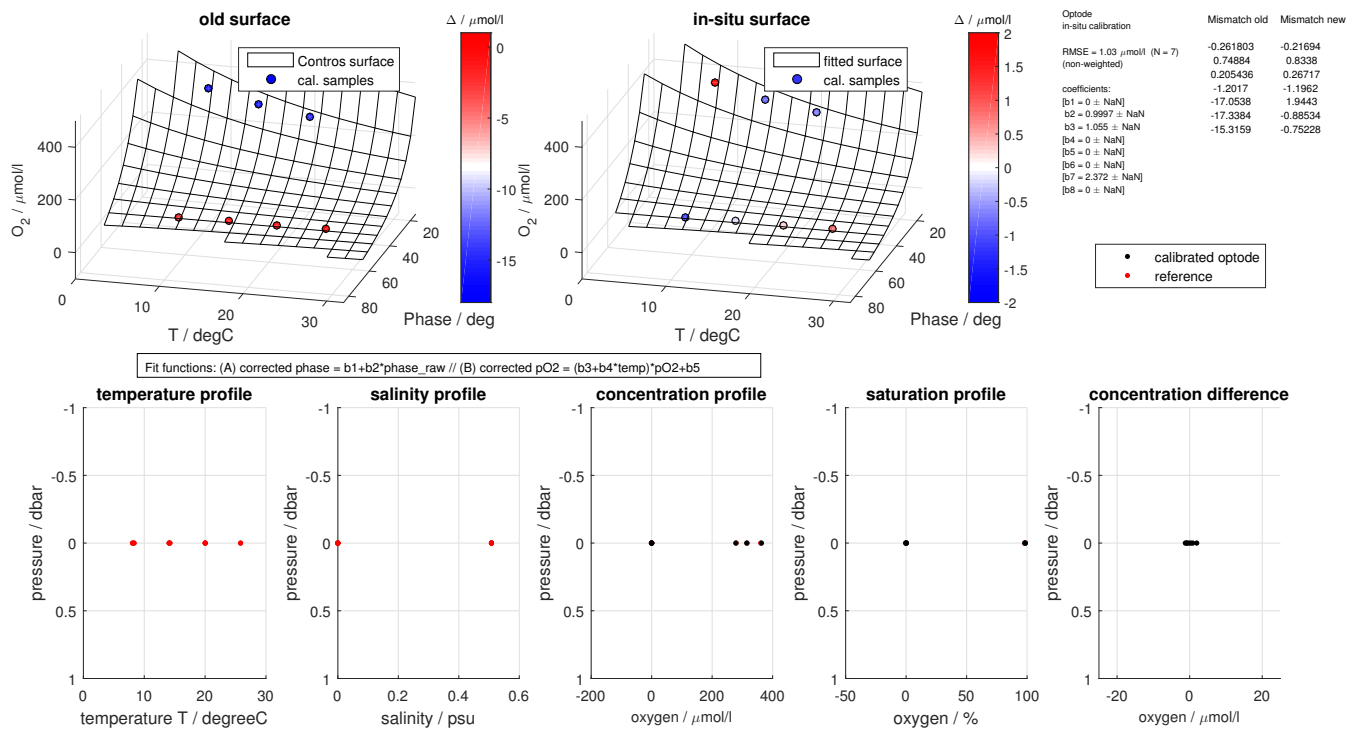


Figure S6: Re-adjustment of HF17-01 from our two-point calibration in the laboratory

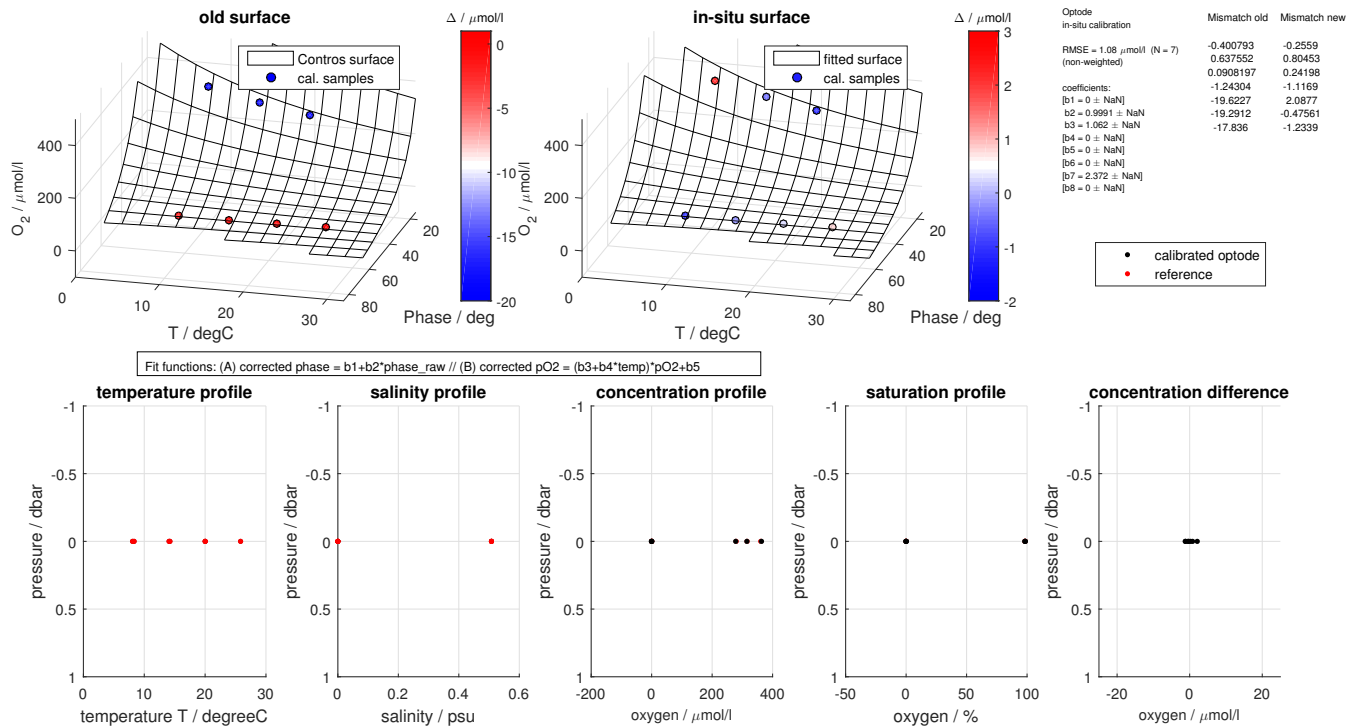


Figure S7: Re-adjustment of HF17-02 from our two-point calibration in the laboratory

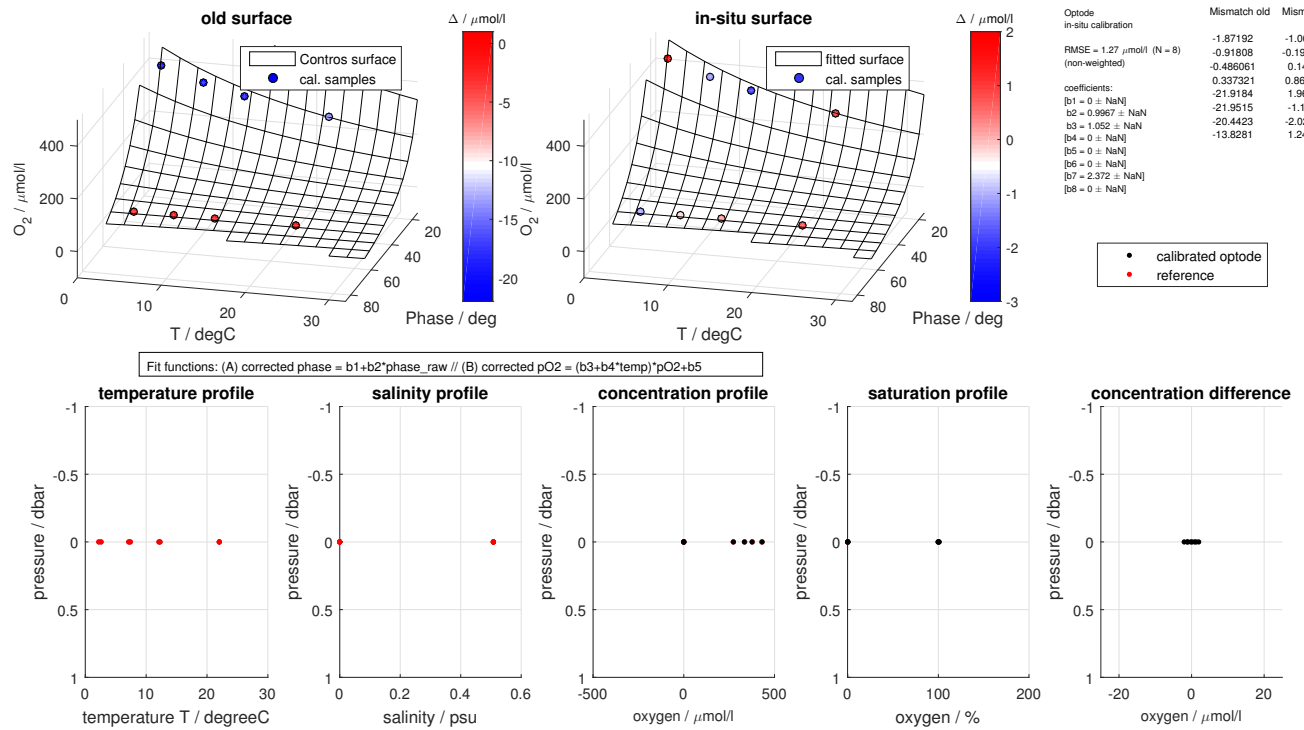


Figure S8: Re-adjustment of HF17-03 from our two-point calibration in the laboratory

17 1.2.2 From field experiments

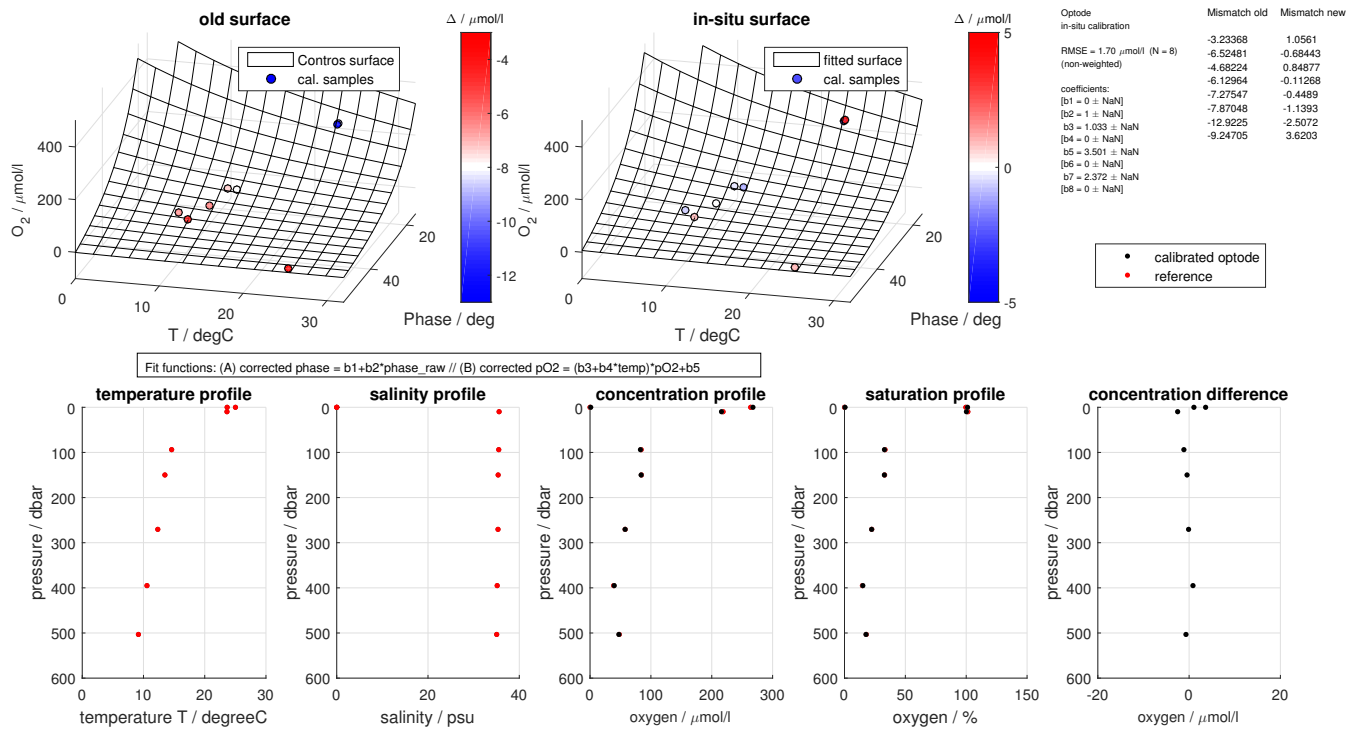


Figure S9: Re-adjustment of HF16-05 inside the original parameter space

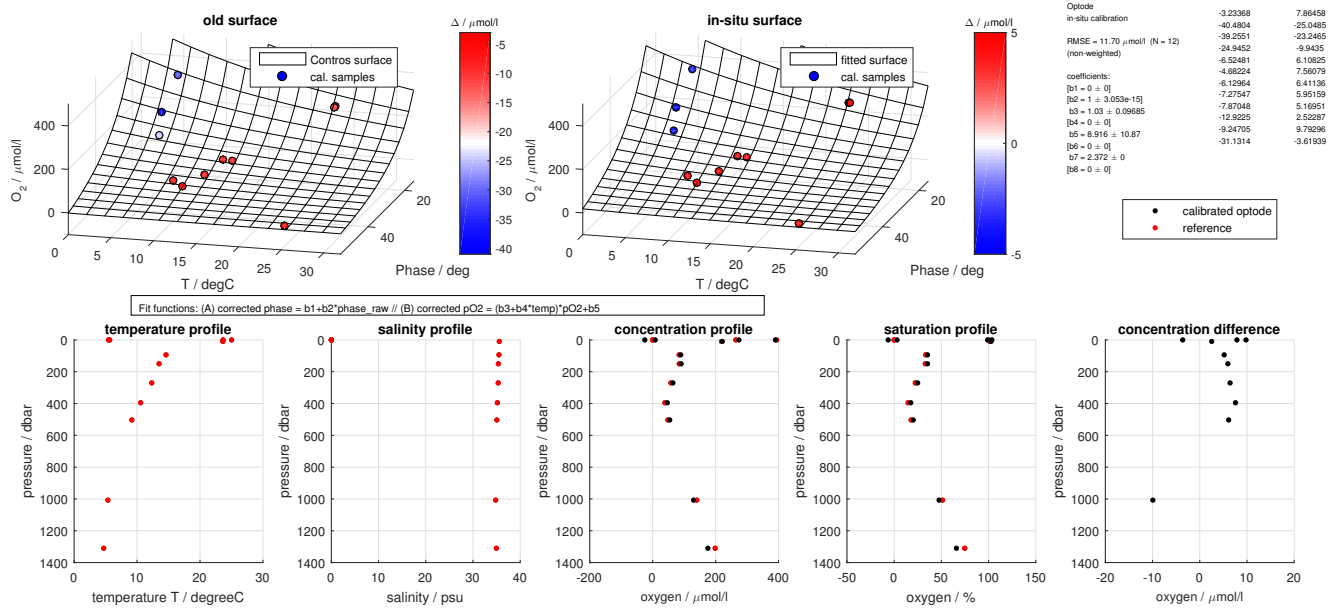


Figure S10: Re-adjustment of HF16-05 inside and outside the original parameter space

18 1.3 Hydrostatic Pressure Dependence

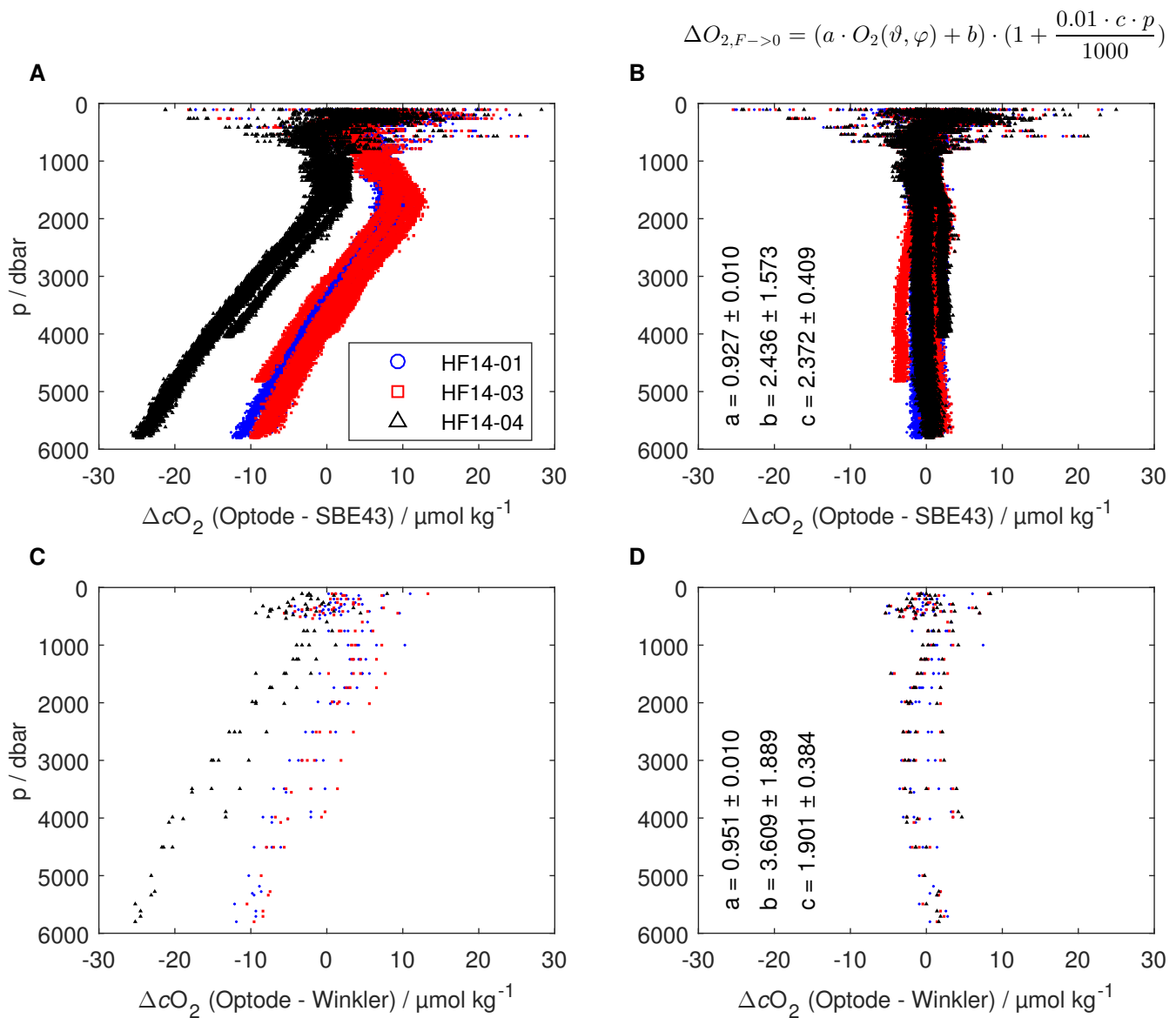


Figure S11: Results for the hydrostatic pressure dependence before (A, C) and after (B, D) applying correction equation (6) of the CONTROS HydroFlash® O₂ optode based on SBE43 (A, B) and Winkler (C, D) reference points. We obtained a slightly lower mean value of variable c using Winkler references samples, but yielded higher mean offsets (Optode - Winkler) taking all deep profiles for depths below 100 m into account.

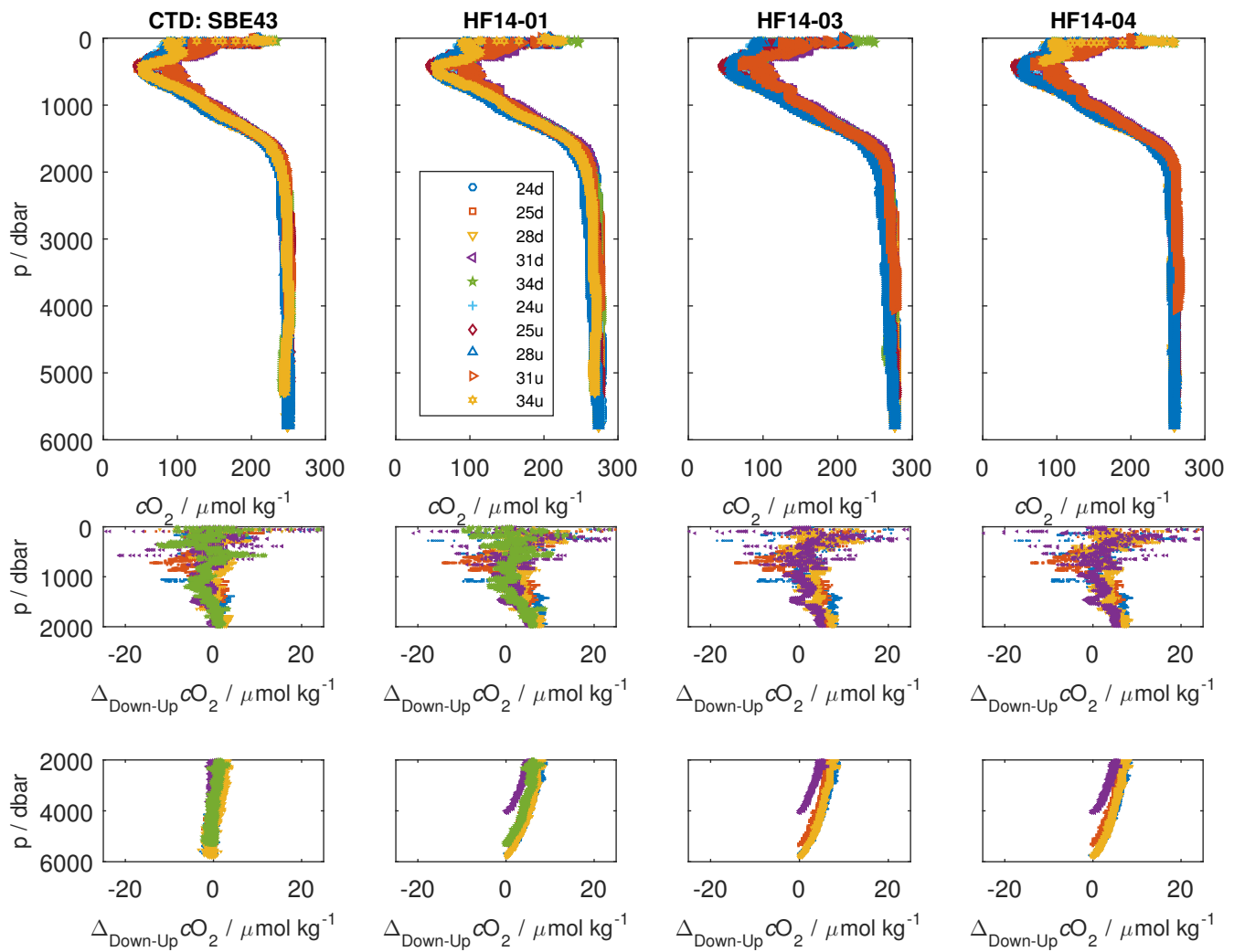


Figure S12: Potential pressure hysteresis of CONTROS HydroFlash[®] O₂ optodes. Given the in situ character of the experiment and the unclear optode behaviour in the upper 100 m, we cannot fully exclude whether the optode experiences pressure hysteresis. This may be supported by the curvature of deep oxygen optode profiles (bottom row) displaying the oxygen concentration difference between downcast and upcast.

19 1.4 Stability Assessment

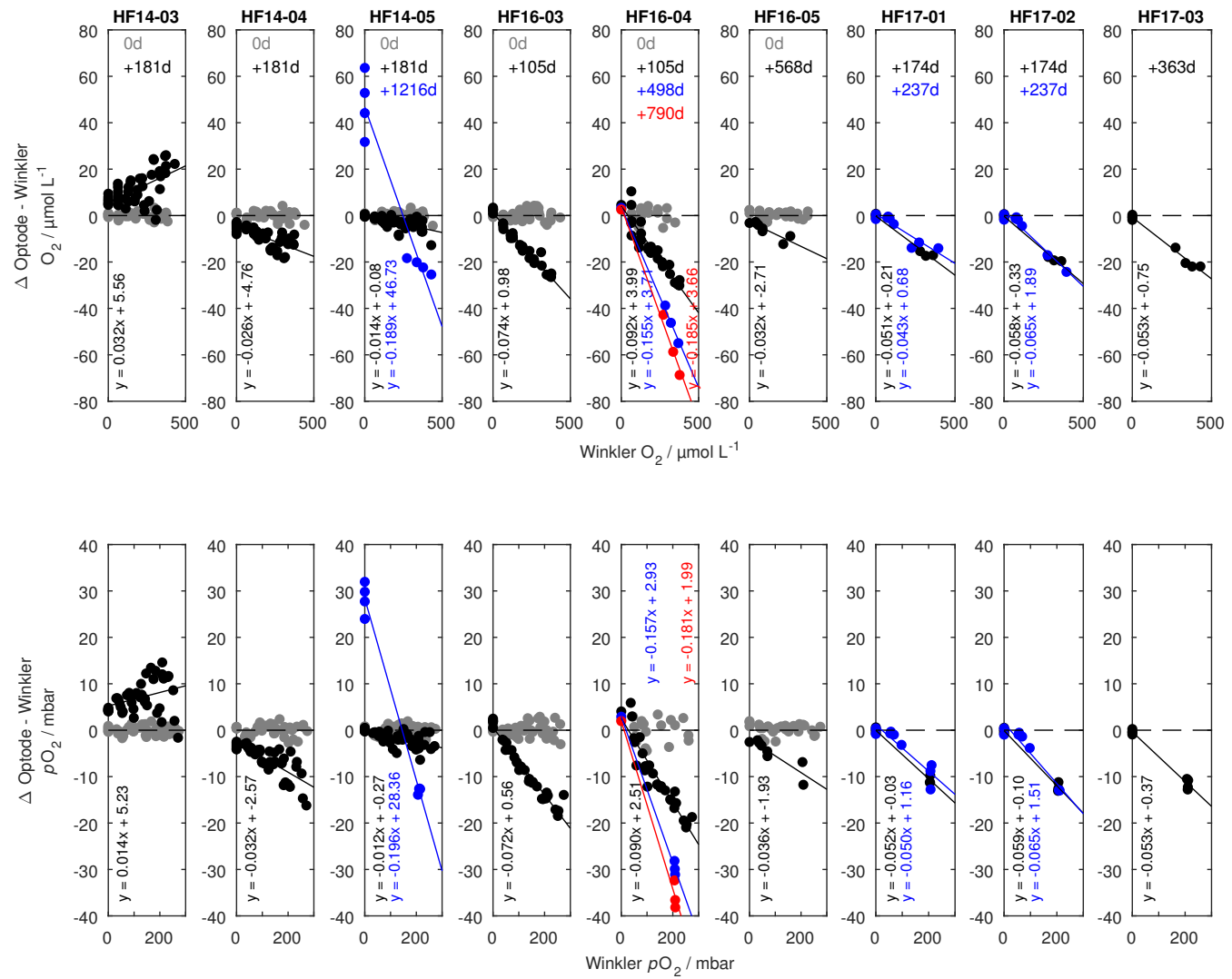


Figure S13: Drift behaviour plots over time of all CONTROS HydroFlash® O₂ optodes used in this study.

20 1.5 Other Evidences from Experiments

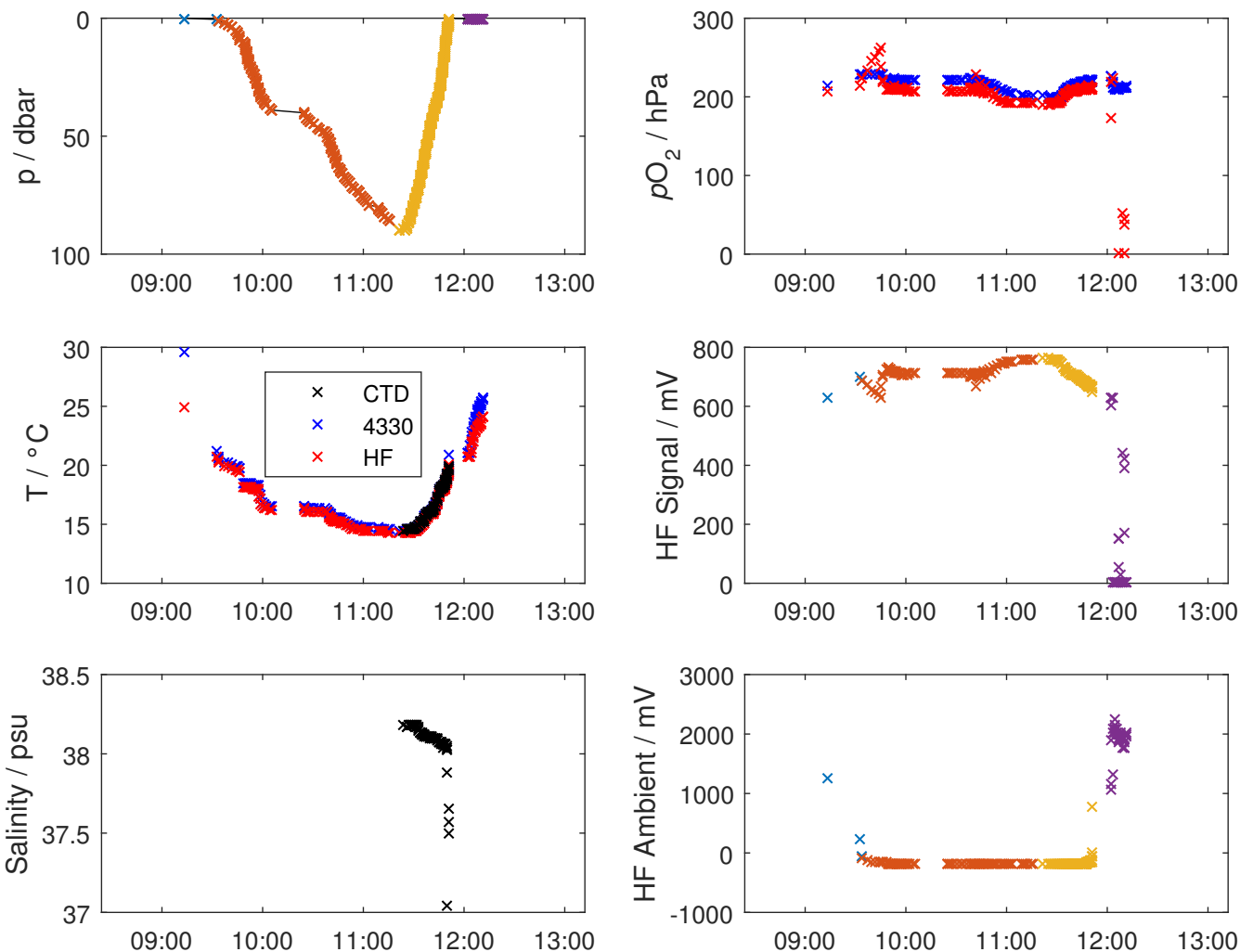


Figure S14: A proof-of-concept implementation of a CONTROS HydroFlash® O₂ optode (HF16-01) on a PROVOR Argo float in collaboration with the Laboratoire d’Océanographie de Villefranche-sur-Mer (LOV): The optode was integrated into the top structure, power supply and data string transmission of the float next to a CTD and 4330 optode yielding data for pressure, temperature, number of measurements, the optodes’ phase shift (converted to pO_2 with temperature and calibration coefficients), signal intensity and ambient light. Data points were obtained during the floats’ cycle, i.e. pre-descent, descent, ascent and surfacing. While all measurements showed normal behaviour before the floats full ascent, the optode revealed a strong sensitivity of the sensor spot when exposed to direct solar irradiation at the surface at about 12:00 pm on 7th June 2016. HF16-01 optode obtained a multi-point calibration (MP3) about 1.5 months before the Argo float deployment, thus optode drift may explain the difference in pO_2 to the 4330.

2 SUPPLEMENTARY TABLES

Table S1. Properties and specifications of the latest CONTROS HydroFlash® O₂ optode (Kongsberg Maritime Contros GmbH, 2019). All sensors used in this study except for HF17-01 -02 and -03 are calibrated at GEOMAR. However, sensors were calibrated individually for temperature and *p*O₂ with a respective calibration sheet.

Property	Description/Specifications
Housing, dimensions	Corrosion-free titanium, cylindrical, 23 mm x 170/197 mm (without/with connector)
Weight	0.17 kg in air, 0.11 kg in water
Operational depth capability	6000 m (standard)
Connector	SubConn MCBH-4M Titanium 4-pin
Supply voltage	6–32 Vdc
Power consumption	Measurement: 0.1 Ws per sample, during stand-by: 0.3 mA
Measuring principle	Dynamic luminescence quenching
Measurement range	0 – 300 mbar <i>p</i> O ₂
Operating temperature	2 °C – 35 °C
Resolution	0.01 mbar or < 0.1 %
Initial accuracy	±1 %
Response time (<i>t</i> _{63%})	<3 s
Sampling rate	≤1 Hz (between every 1 second to 24 hours)
Wake-up time	3–4 s, if data logger is empty
Data logger	Capable of logging approx. 2 million sets of data
Data interface	RS-232C
Data format	ASCII
Battery pack	External battery pack CONTROS HydroB® Flash

Table S2. Inventory matrix of calibrated CONTROS HydroFlash® O₂ and reference optodes used in this study. The table displays several sensor versions (including our test optodes HF14-06, HF15-05 and HF15-12 not yielding quantitative results), performance characteristics dependencies and respective field applications used over the course of this study. Legend for top column: Ox — oxygen dependence, S — salinity dependence, p — hydrostatic pressure dependence, Drift — stability assessment, τ — time dependence, UW — underway measurements in a flow-through box, CTD — profiling application on a rosette sampler in the water column, CVOO — mooring application at the Cabo Verde Ocean Observatory, Air — air measurements with strong sunlight on the top deck during M116, Float — Argo float test profile, cref — Chapter reference in the main manuscript. The symbol (x) denotes the optode facing the parameter throughout its lifetime, but not contributing substantially to the respective key sensor performance data evaluation.

Optode Letter Code	Ox	S	p	Drift	τ	UW	CTD	CVOO	Air	Float	cref
DO-1,-2,-3	-	-	-	-	x	-	-	-	-	-	3.6.1
HF14-01	x	x	x	-	-	x	x	-	x	-	3.2, 3.4, 3.6.2, 3.7
HF14-03	x	x	x	x	-	-	x	-	x	-	3.2, 3.3, 3.4, 3.5.1, 3.6.2, 3.7
HF14-04	x	x	x	x	-	-	x	-	x	-	3.2, 3.3, 3.4, 3.5.1, 3.6.2, 3.7
HF14-05	x	x	-	x	-	x	x	-	-	-	3.2, 3.3, 3.5.1
HF14-06	-	-	-	-	-	-	(x)	-	-	-	(preliminary tests)
HF15-05	-	-	-	-	-	-	-	(x)	-	-	(preliminary tests)
HF15-12	-	-	-	-	-	-	-	(x)	-	-	(preliminary tests)
HF16-01	x	(x)	-	-	-	-	-	-	-	x	3.2, 3.7
HF16-02	x	-	-	-	-	-	-	-	-	-	3.2
HF16-03	x	(x)	(x)	x	-	-	(x)	x	-	-	3.2, 3.5.2
HF16-04	x	(x)	(x)	x	-	-	-	-	-	-	3.2, 3.5.1
HF16-05	x	x	(x)	x	-	-	x	x	-	-	3.2, 3.3, 3.5.1, 3.5.2
HF17-01	x	-	-	x	-	-	x	x	-	-	3.2, 3.5.2
HF17-02	x	-	-	x	-	-	x	x	-	-	3.2, 3.5.2
HF17-03	x	-	-	x	-	-	-	-	-	-	3.2, 3.5.2
4330-1082	x	x	-	-	-	x	-	-	-	-	3.2, 3.3
4330-1277	x	-	-	-	-	-	-	-	-	-	3.2
4330-2238	x	-	-	-	-	-	-	-	-	-	3.2
SBE 63-392	x	-	-	-	-	-	-	-	-	-	3.2

Table S3. Mean chemical composition and ionic strength (defined as $I = \frac{1}{2} \sum_{i=1}^n c_i \cdot z_i^2$) of standard seawater (at $T = 25^\circ\text{C}$, $S = 35$, $\rho_{T=25^\circ\text{C}} = 0.997048$, according to Dickson et al. (2007, chap. 5).

Species	$M [\frac{g}{mol}]$	$M [\frac{mg}{mol}]$	z_i	$c [\frac{mol}{kg\text{H}_2\text{O}}]$	$c_i \cdot z_i^2$
Cl^-	35.453	35453	1	0.56576	0.56576
SO_4^{2-}	96.06	96060	2	0.02927	0.11708
Br^-	79.904	79904	1	0.00087	0.00087
F^-	18.998403	18998.403	1	0.00007	0.00007
Na^+	22.989769	22989.769	1	0.48616	0.48616
Mg^{2+}	24.305	24305	2	0.05475	0.219
Ca^{2+}	40.078	40078	2	0.01065	0.0426
K^+	39.0983	39098.3	1	0.01058	0.01058
Sr^{2+}	87.62	87620	2	0.00009	0.00036
B(OH)_3	61.83	61830	0	0.00033	0
B(OH)_4^-	78.84	78840	1	0.0001	0.0001
CO_2	44.01	44010	0	0.00001	0
HCO_3^-	61.0168	61016.8	1	0.00183	0.00183
CO_3^{2-}	60.008	60008	2	0.00027	0.00108
OH^-	17.008	17008	1	0.00001	0.00001
NH_4^+	17.031	17031	1	0	0
BrO_3^-	127.901	127901	1	0	0
NO_3^-	62.0049	62004.9	1	0	0
NO_2^-	46.005	46005	1	0	0
PO_4^{3-}	94.9714	94971.4	3	0	0
$\sum 1.16075$					
$I \quad 0.72275$					
$S \quad 35$					

Table S4: Chemical composition data of tab water from local municipal (Stadtwerke Kiel AG) supply locations at a) Schulensee and Schwentinetal, and b) Pries and Wik. The calculations of salinity for a) and b) result from ionic strength (defined as $I = \frac{1}{2} \sum_{i=1}^n c_i \cdot z_i^2$) and conductivity C of all four datasets. We used an average salinity value of $S = 0.508$ based on ionic strength for the final fit reference points at 100 % saturation levels during lab calibrations of CONTROS HydroFlash® O₂ optodes in this study. Note: Tab water composition data as of January 2019 was available through <https://www.stadtwerke-kiel.de/swk/de/produkte/privatkunden/wasser/qualitaet/qualitaet.jsp>.

a) Species	Schulensee			Schwentinetal		
	$\beta_i [\frac{mg}{L}]$	$c [\frac{mol}{kgH_2O}]$	$c_i \cdot z_i^2$	$\beta_i [\frac{mg}{L}]$	$c [\frac{mol}{kgH_2O}]$	$c_i \cdot z_i^2$
Cl ⁻	20	0.000562462	0.000562462	63	0.001771755	0.001771755
SO ₄ ²⁻	9	9.34149E-05	0.000373659	51	0.000529351	0.002117404
Br ⁻	0	0	0	0	0	0
F ⁻	0.19	9.97132E-06	9.97132E-06	0.21	1.10209E-05	1.10209E-05
Na ⁺	16.5	0.000715592	0.000715592	48.3	0.002094733	0.002094733
Mg ²⁺	10.1	0.000414326	0.001657303	11.7	0.000479961	0.001919846
Ca ²⁺	92	0.002288747	0.009154989	112	0.002786301	0.011145204
K ⁺	2.78	7.08929E-05	7.08929E-05	3.14	8.00733E-05	8.00733E-05
Sr ²⁺	0	0	0	0	0	0
B(OH) ₃	0	0	0	0	0	0
B(OH) ₄ ⁻	0	0	0	0	0	0
CO ₂	12	0.00027186	0	13	0.000294515	0
HCO ₃ ⁻	331.9	0.005423428	0.005423428	353.3	0.005773116	0.005773116
CO ₃ ²⁻	0	0	0	0	0	0
OH ⁻	0	0	0	0	0	0
NH ₄ ⁺	0.15	8.78147E-06	8.78147E-06	0.02	1.17086E-06	1.17086E-06
BrO ₃ ⁻	0.001	7.79547E-09	7.79547E-09	0.001	7.79547E-09	7.79547E-09
NO ₃ ⁻	13.9	0.000223514	0.000223514	1.92	3.08739E-05	3.08739E-05
NO ₂ ⁻	0.019	4.11779E-07	4.11779E-07	0.005	1.08363E-07	1.08363E-07
PO ₄ ³⁻	0.09	9.44856E-07	8.50371E-06	1	1.04984E-05	9.44856E-05
	$\sum 0.01008$			$\sum 0.01386$		
	I			I		
	S			S		
	$C_{T=25^\circ C} [\frac{\mu S}{cm}]$			$C_{T=25^\circ C} [\frac{\mu S}{cm}]$		
	$S_{f=sal78sw}$			$S_{f=sal78sw}$		
b)	Pries			Wik		
Cl ⁻	15	0.000421846	0.000421846	123	0.00345914	0.00345914
SO ₄ ²⁻	1.9	1.97209E-05	7.88837E-05	2.3	2.38727E-05	9.54908E-05
Br ⁻	0	0	0	0	0	0
F ⁻	0.22	1.15457E-05	1.15457E-05	0.16	8.3969E-06	8.3969E-06
Na ⁺	16.6	0.000719929	0.000719929	60.8	0.002636848	0.002636848
Mg ²⁺	10.2	0.000418428	0.001673712	16.3	0.000668664	0.002674657
Ca ²⁺	72	0.001791194	0.007164774	108	0.00268679	0.010747161

Table S4: (continued)

Species	$\beta_i \left[\frac{mg}{L} \right]$	$c \left[\frac{mol}{kg_{H_2O}} \right]$	$c_i \cdot z_i^2$	$\beta_i \left[\frac{mg}{L} \right]$	$c \left[\frac{mol}{kg_{H_2O}} \right]$	$c_i \cdot z_i^2$	
K ⁺	3.02	7.70132E-05	7.70132E-05	4.96	0.000126485	0.000126485	
Sr ²⁺	0	0	0	0	0	0	
B(OH) ₃	0	0	0	0	0	0	
B(OH) ₄ ⁻	0	0	0	0	0	0	
CO ₂	9.1	0.000206161	0	16	0.000362481	0	
HCO ₃ ⁻	283.7	0.004635814	0.004635814	366.7	0.005992079	0.005992079	
CO ₃ ²⁻	0	0	0	0	0	0	
OH ⁻	0	0	0	0	0	0	
NH ₄ ⁺	0.079	4.62491E-06	4.62491E-06	0.0029	1.69775E-07	1.69775E-07	
BrO ₃ ⁻	0.001	7.79547E-09	7.79547E-09	0.001	7.79547E-09	7.79547E-09	
NO ₃ ⁻	1.36	2.1869E-05	2.1869E-05	2.58	4.14868E-05	4.14868E-05	
NO ₂ ⁻	0.015	3.25089E-07	3.25089E-07	0.012	2.60071E-07	2.60071E-07	
PO ₄ ³⁻	0.18	1.88971E-06	1.70074E-05	0.03	3.14952E-07	2.83457E-06	
	$\sum 0.00833$			$\sum 0.01601$			
	<i>I</i>	0.00741		<i>I</i>	0.01289		
	S	0.359		S	0.624		
	C _{T=25°C} [$\frac{\mu S}{cm}$]	462		C _{T=25°C} [$\frac{\mu S}{cm}$]	902		
	S _{f=sal78sw}	0.223		S _{f=sal78sw}	0.443		
	Mean values a) & b)						
	$\bar{I} = 0.010 \pm 0.002$						
	$\bar{S} = 0.508 \pm 0.112$						
	$\bar{C}_{T=25°C} = 675.750 \pm 174.835 \frac{\mu S}{cm}$						
	$\bar{S}_{f=sal78sw} = 0.330 \pm 0.087$						

REFERENCES

- 21 Dickson, A., Sabine, C., and Christian, J. (2007). Guide to best practices for ocean CO₂ measurements.
 22 PICES Special Publication 3 , 191 pp.
 23 Kongsberg Maritime Contros GmbH (2019). *CONTROS HydroFlash Datasheet*